A study of precipitation hardening of commercial Al-9 wt % Si alloy

M. KACZOROWSKI, M. W. GRABSKI*, J. SAWICKI,
P. MURZA–MUCHA
*Institute of Casting, Welding and Bulk Metal Forming, and *Institute of Materials Science and Engineering, Technical University of Warsaw, Narbutta 85, 02-524 Warsaw, Poland*

Structural and morphological investigations of the processes occurring in Al–9 wt % Si silumin during isothermal ageing at high temperatures were performed using hardness measurements and electron microscopic observations. It was established that the alloy achieved maximum hardness after being aged for 2.7×10^3 sec at a temperature of about 463 K. During this time, formation of clusters of supersaturating atoms, probably of spherical symmetry, was observed, and which, as the ageing time lengthened, assumed the form of needles (GP zones). It is suggested that GP zones contain "foreign" atoms (impurities, e.g. Fe, Mn, Na) which may tend to increase the stability of these zones. During continued ageing, in the period between 1.1×10^4 and 2.2×10^4 sec, excess silicon precipitates appeared. These precipitates increased in size progressively as the ageing time was increased, whereas the GP zones, after reaching a certain magnitude, remained unchanged. The change GP zones $\rightarrow \beta'$-phase rod-like precipitates occurs after ageing for approximately 8.6×10^4 sec. Differences between the course of ageing in Al–9 wt % Si silumin and in (after supersaturation) single-phase alloys from a pseudo-binary Al–Mg$_2$Si system, are discussed.

1. Introduction

The most popular casting alloys being used in metallurgy, in addition to cast irons, are aluminium and silicon alloys, commonly called silumins. Their wide practical application is the effect of their exceptionally good castability and fairly good mechanical properties. The latter can be increased by thermal treatment which consists in solution treating and ageing the casting at high temperatures.

The phase changes occurring during the ageing of alloys in the Al–Mg–Si system have been the object of intensive study [1–9]. This has shown that the sequence of decomposition of a supersaturated solid solution is as follows [10–12]: GP zones of needle-like or spherical morphology $\rightarrow$ rod-like β'-phase precipitates $\rightarrow$ platelet equilibrium precipitates of the compound Mg$_2$Si. It has also been found that the sequence of decomposition of a supersaturated solid solution, as well as its mechanical properties, are essentially

dependent on thermal history. Particular attention was given to the structural changes occurring during two-step ageing [13, 14]. It was also found that an addition of Fe and Si affects the density of the precipitates being formed, thus increasing the strength properties of the alloy [15]. Excess silicon also accelerates the dispersion hardening process [16]. It was finally observed that the course of the precipitation process was essentially affected by excess vacancies remaining during solution treatment [17].

At this point it should be noted that the work referred to above concern alloys from a pseudo-binary Al–Mg$_2$Si system, in which the quantity of Mg$_2$Si varied within the limits 0.4 to 1.75%, with the excess silicon being 0.28 wt % maximum. So far there have been no data given in the literature to discuss and illustrate the structural changes accompanying the dispersion hardening process occurring in Al–Si casting alloys containing a number of additions (Mg, Mn, Fe and others) in

which the excess silicon quantity exceeds considerably the value investigated to date (0.28%).

The purpose of the present study was to investigate the phase changes occurring during the course of ageing of commercial Al–9 wt % Si silumin, and in particular to determine whether there occur differences between precipitation in the casting alloy and that in the alloys used for plastic treatment.

2. Experimental

The test material was samples cut from a suction collector cast of Al–9 wt % Si silumin of the composition: Si 8.5 to 9.5%, Mg 0.2 to 0.4%, and Mn 0.25 to 0.5%. In accordance with the Polish Standards, the alloy could contain additions in the following quantities: Fe 0.5 to 1.0%, Zn 0.2%, Cu 0.3%, and Ti 0.15%.

Before pouring into the metal mould, whose temperature was 576 K, the liquid alloy was inoculated with a mixture of the salts: 40 wt % NaCl + 40 wt % NaF + 20 wt % KCl. The casting obtained was annealed for 3.6×10^3 sec (1 h) at approximately 833 K and subsequently quenched in water at 291 K. Following supersaturation, the alloy was aged at $\sim 463 \, K^*$ for $\tau = 2.7 \times 10^3, 5.4 \times 10^3$, 1.08×10^4, 2.16×10^4, 4.32×10^4 and 8.64×10^4 sec (0.75, 1.5, 3.0, 6.0, 12.0, and 24 h). For the heat treated alloy, hardness measurements and electron microscopic observations were carried out. In the hardness test, the Brinell and Vickers methods were applied.

In the Brinell method, a small sphere, 2.5 mm diameter, and a pressure of 30 kg was used, and in the Vickers method, a diamond pyramid with an obtuse angle of 2.37 rad (136°), and a pressure force of 5 kg.

Samples for the electron microscopic investigations were cut from a cylinder, 3 mm diameter, by the abrasive cutting method. Discs 0.1 mm thick were electrolytically thinned by the single-jet method [18]. The foils prepared were observed in a Philips EM 300 transmission electron microscope equipped with a goniometer stage, operating at an accelerating voltage of 100 kV.

3. Results
3.1. Hardness tests
Fig. 1 shows the course of changes in hardness as a function of ageing time. The diagram indicates
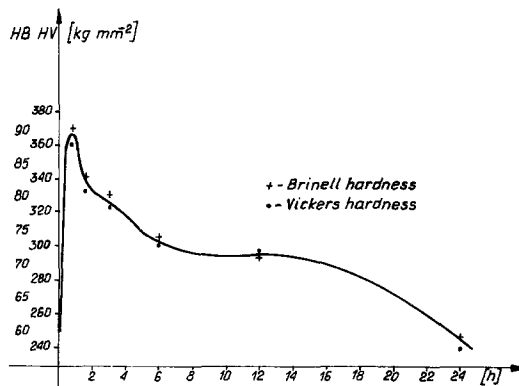

Figure 1 Hardness curve for Al–9 wt % Si alloy as a function of ageing time at 463 K.

that the hardness achieves a maximum value after a time of approximately 2.7×10^3 sec. As ageing time is increased, hardness decreases gradually, and after 8.6×10^3 sec achieves a value close to that which the alloy possessed immediately after solution treatment. The curve shown differs basically from those presented in the publications concerning alloys which, after solution treatment, are single-phase [16]. This difference relates to the time after which maximum alloy hardness is achieved for a given ageing temperature. For alloys of Al–0.8 wt % Mg_2Si composition aged at a temperature of 448 K, maximum hardness was obtained only after approximately 9×10^4 sec (25 h).

3.2. Electron microscopic investigations
Fig. 2 shows the structure of Al–9 wt % Si silumin, supersaturated and kept for 30 days at 288 K. The figure shows dislocation loops and fairly numerous dislocations. No effects were observed, however, which might indicate the initiation of a precipitation process. This observation is consistent with earlier findings [19], according to which the hardening process practically does not take place in Al–Si casting alloys during natural ageing. The relatively large number of dislocations in foils after solution treatment compared with the same number in foils aged at a higher temperature, is probably the result of deformations taking place during the cutting of the sample.

Fig. 3 shows alloy structure after ageing for 2.7×10^3 sec at 463 K, observed in a dark field. A characteristic contrast is seen, which was observed neither in foils after solution treatment

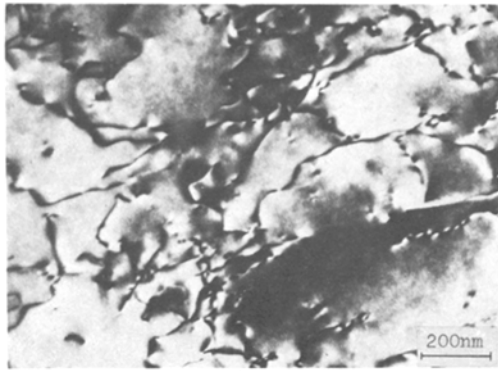*Heat treatment was carried out under industrial conditions.

Figure 2 Structure of supersaturated silumin aged for 30 days at 283 K.

Figure 4 Needle-shaped GP zones in the alloy aged for 5.4×10^3 sec at 463 K.

nor after prolonged ageing times, despite the foils being inclined within a large angular range. This contrast is similar to that observed during spinoidal decomposition. It might, therefore, be reasonably suggested that this is the early stage of formation of GP zones, and it appears that the concentrations have a spherical rather than a needle-like morphology — a fact which is apparently consistent with the observations made by Cordier and Grühl [20] and by Smith [21].

The alloy structure after ageing for 5.4×10^3 sec is shown in Fig. 4, in which GP zones of needle-like morphology are clearly visible. Somewhat surprising is a strong strain contrast seen around the GP zones [22].

The GP zones are $30 \, nm \times 50 \, nm$ in size. An analysis of microscopic and diffraction pictures shows that the zones are situated parallel to $\langle 0\,1\,0 \rangle$ direction, which is consistent with literature data. The GP zones increase as the ageing time is increased, which is illustrated in Fig. 5.

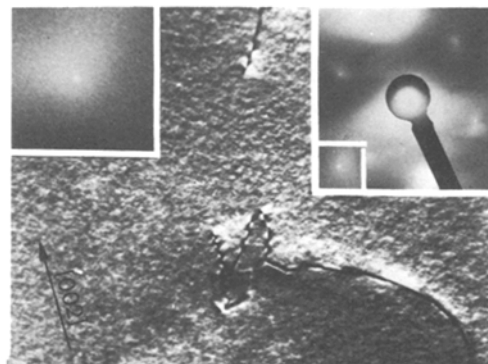The structure of Al–9 wt % Si silumin after

being aged for 2.16×10^4 sec, observed in a dark field is shown in Fig. 6. Needle-like Guinier–Preston zones are seen distributed in three mutually perpendicular $\langle 0\,1\,0 \rangle$ directions.

At many points silicon precipitates can be observed, having a different, although most frequently spheroidal, morphology. The appear-
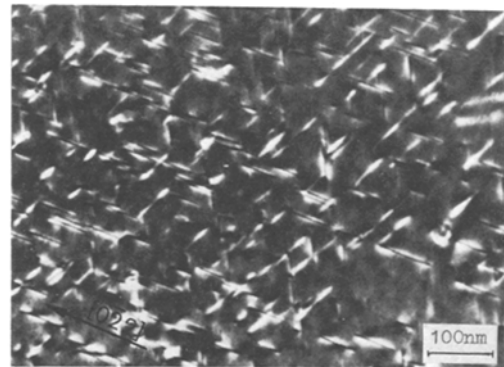
Figure 5 Structure of silumin aged for 1.08×10^4 sec (dark-field electron micrograph).

Figure 3 Dark-field electron micrograph of the alloy aged for 2.7×10^3 sec at 463 K.

Figure 6 GP zones situated in three mutually perpendicular directions, observed in foil aged for 2.16×10^4 sec at 463 K.

2783

ance of excess silicon precipitates is accompanied by the occurrence of spots on the circumference of the rings. Such a diffraction pattern suggests that the orientation of these precipitates in relation to the aluminium matrix is accidental. The weak intensity of the spots prevented their being registered on the electronogram.

After ageing for 4.32×10^4 sec, silicon precipitates achieved considerable dimensions and became thicker. It is worth noting that some of these precipitates, which were needle-shaped, became equal to, and sometimes greater than, the GP zones.

Spots from Si are also seen in the diffraction patterns. It appears that some of the zones were transformed into rod-like β'-phase precipitates. However, no spots from this phase were observed.

The last micrograph (Fig. 7) shows silumin structure after ageing for 8.64×10^4 sec. Rod-like β'-phase precipitates distributed in three mutually perpendicular $\langle 0\,1\,0 \rangle$ directions are seen. These precipitates have, until recently, been given the stoichiometric formula Mg_2Si and fcc structure with the lattice parameter $a = 0.642 \pm 0.007$ nm. However, Jacobs [9] has shown recently that phase precipitates have a hexagonal structure with lattice parameters $a = 0.705 \pm 0.005$ nm, and $c = 0.405 \pm 0.001$ nm.

4. Discussion

On the basis of the hardness tests performed, it was found that Al–9 wt % Si silumin solution treated at a temperature $T = 833$ K and aged at a temperature of 463 K achieves the maximum hardening after a time $\tau = 2.7 \times 10^3$ sec. It is seen from electron microscopic observations that in this period a specific tweed-like contrast appears

Figure 7 Rod-like β' precipitates in Al–9 wt % Si silumin, lying in $\langle 0\,1\,0 \rangle$ directions.

in the microscopic pictures, characteristic of the structures obtained as a result of spinodal decomposition. This is supported by observations of diffuse scattering around primary diffraction spots which is characteristic for composition modulations of non-specific wavelength. With prolonged ageing time, the clusters are most probably rearranged into the needle-like GP zones. The lack of streaks on the diffraction patterns indicates that the zones are then too big, or that distribution of atoms inside the zones is similar to that predicted by Tomann's model [23].

The next point of interest is the strong strain contrast accompanying the zones of needle-like symmetry (Fig. 5). As already mentioned, according to previous papers, deformation of the matrix amounts to a bare 2% and could by no means be the cause of such a strong effect [24]. It should, however, be noted that such deformation is only in the case when it is assumed that an ordered arrangement of atoms in the zones is distributed in the form of chains [25]. If the presence of foreign atoms such as Fe, Mn, which can undoubtedly be incorporated into the chains, is taken into account it is expected that such atoms will disturb the order within the zone, and consequently give rise to a greater misfit between that zone and the surrounding matrix. Such an explanation seems to be sufficiently logical, but it would, nevertheless, require confirmation in the form of the establishment of the chemical composition of the particular zone, which unfortunately is rather difficult. From the previous conclusion it follows that the composition in question is fairly complicated, and should consequently be written in the form $Mg_x Si_y Me_z$, which Me = metal (e.g. Fe, Cu, Mn), and x, y, z = contributions of individual atoms in the zone.

As already mentioned in Section 1, excess silicon, although it does not change the character of the transformation, does cause considerable qualitative changes which are noticeable even with Si quantities of 0.28% [16]. In the case of Al–9 wt % Si silumin, the quantity of excess silicon is considerably higher, and its influence therefore appropriately stronger. In the interpretation of the results obtained from hardness tests performed by the Vickers method, the eutectic silicon presented an additional difficulty. It was established that whereas hardness measured by the Brinell method corresponded to appropriate literature data, hardness in the HV scale was

considerably higher. In view of the identical shape of the HB and HV hardness curves as a function of the ageing time, the results obtained by the Vickers method could not be accidental, and more so that the spread of HV hardness values was insignificant. Differences between HV scale hardness given in the publications for single-phase Al–Mg$_2$Si alloys (after solution treatment) and the hardness obtained in this work can be explained by the presence of eutectic silicon which constitutes, as it were, "the reinforcement" of the metallic matrix of the solid solution.

The next problem of interest is the process of precipitation from the supersaturated solution of excess silicon which appears considerably later (after $\sim 2.16 \times 10^4$ sec) than the GP zones. If it is taken into account that in order for the critical nucleus to be formed, even during heterogeneous nucleation, it is necessary to provide an appropriate activation energy, whereas in the light of the present views, formation of GP zones is believed to occur spontaneously as a result of spinodal decomposition [26]; the time of formation of zones is, therefore, determined by the velocity of diffusion of atoms, or, to be exact, of dissolved atom–vacancy pairs.

In addition to structure defects such as excess vacancies, dislocations, grain boundaries, if the presence of α/Si interphase boundaries, and also the existence in the alloy of a series of additions and impurities are taken into account, it can be expected that formation of GP zones in Al–9 wt % Si silumin will occur earlier than in the case of cold-worked Al–Mg$_2$Si alloys. It also appears that the acceleration of the hardening process is considerably affected by the structure of the casting, in contrast to that of the plastically treated alloy.

"Delayed" silicon precipitation connected with the necessity of providing an appropriate activation energy, may also be caused by the fact that considerable part of vacancies are used earlier during the formation of the zones. It should, however, be noted that, after the origination of Si precipitates, these precipitates increase in size rapidly, some of them (morphologically comparable) becoming greater than the rod-like β'-phase precipitates. This fact may have the following explanation. The growth of silicon precipitates occurs continuously by incorporation of Si atoms, whose number is proportional to the ageing time. This process will continue until the concentration of silicon atoms supersaturating the matrix achieves an equilibrium. By contrast, the growth of needle-like GP zones continues until the moment when conditions are formed for β'-phase precipitation. Most frequently formation of the metastable phase is preceded by dissolution of the zones. However, since the zones may comprise "foreign" atoms (e.g. Mn, Fe, Na, Cu) which may have a stabilizing effect on the zones, it should be taken into account that, in order for them to be dissolved, an appropriately greater activation energy will have to be provided than that required in the absence of impurities. The correctness of the above reasoning is apparently confirmed by the shape of the hardness curve as a function of ageing time which clearly shows a characteristic "plateau" within the ageing range from 1.8×10^4 to 5.4×10^4 sec (5 to 15 h).

5. Conclusions

The following conclusions can be drawn from the results obtained and the above discussion:

(1) the dispersion hardening process of Al–9 wt % Si casting alloys is, if not qualitatively, quantitatively different than in the case of cold-worked Al–Mg$_2$Si alloys;

(2) clusters appearing during the early ageing stages have a spherical rather than a needle-like symmetry, but a final statement would require a more accurate electron microscopic study;

(3) earlier achievement of maximum hardness by the alloy compared with these alloys which after supersaturation are single-phase, may be the result of: (a) a greater number of excess vacancies in the casting alloy, (b) a greater number of α/Si interphase boundaries, (c) easier formation of GP zones because of the presence of impurities, or (d) a different structure of the casting alloy compared with that of the plastically treated alloy;

(4) a strong strain contrast around the zones observed in electron microscopic micrographs is connected with the disturbance of the ordered structure by "foreign" atoms situated in the casting alloy.

References

1. T. HIRATA and S. MATSUO, *Trans. Jap. Inst. Metals* **13** (1972) 231.
2. R. C. DORWARD, *Met. Trans.* **4** (1973) 507.

3. Y. MURU KAMI, O. KAWANO, S. KOMATSU, T. OHNISHI and T. NAKAZAWA, *Trans. Jap. Inst. Metals* 9 (suppl.) (1969) 349.
4. G. W. LORIMER and R. B. NICHOLSON, *Acta Met.* 14 (1966) 1009.
5. C. PANSERI and T. FEDERIGHI, *J. Inst. Metals* 94 (1966) 99.
6. J. N. DOWLING and J. W. MARTIN, *Acta Met.* 24 (1976) 1147.
7. A. CZIRÁKI, I. KOVÁCS and E. NAGY, *Phys. Stat. Sol. (a)* 7 (1971) 245.
8. E. KORNGIEBEL, H. LÖFFLER and W. OETTEL, *ibid* 30 (1975) 125.
9. M. H. JACOBS, *Phil. Mag.* 26 (1972) 1.
10. A. SAULNIER and P. MIRAND, *Mem. Sci. Rev. Met.* 57 (1960) 91.
11. G. THOMAS, *J. Inst. Metals* 90 (1961–62) 57.
12. A. LUTTS, *Acta Met.* 9 (1961) 577.
13. D. W. PASHLEY, J. W. RHODES and A. SEND-OREK, *J. Inst. Metals* 94 (1966) 41.
14. D. W. PASHLEY, M. H. JACOBS and I. T. WIETZ, *Phil. Mag.* 16 (1967) 51.
15. J. LENDVAI, I. KOVÁCS and E. NAGY, *Phys. Stat. Sol. (a)* 14 (1972) 83.
16. S. CERESARA, E. DI RUSSO, P. FIORINI and A. GIARDA, *Mat. Sci. Eng.* 5 (1969–70) 220.
17. J. LENDVAI, T. UNGÁR and I. KOVÁCS, *ibid* 16 (1974) 85.
18. M. A. DEWEY, T. G. LEWIS, *J. Sci. Instrum.* 40 (1963) 385.
19. A. P. GULAYEV, "Metallovedenye" (Mir, Moskwa, 1968) p. 538.
20. H. CORDIER, W. GRÜHL, *Z. Metallk.* 56 (1965) 669.
21. W. F. SMITH, *Met. Trans.* 4 (1973) 2435.
22. P. HIRSCH, A. HOWIE, R. NICHOLSON, D. W. PASHLEY and W. J. WHELAN, "Electron Microscopy of Thin Crystal", (Butterworths, London, 1965) Ch. 14.
23. V. A. PHILIPS, *Acta Met.* 21 (1973) 291.
24. G. THOMAS, "Electron Microscopy and Strength of Crystals", edited by G. Thomas and J. Washburn (Interscience, New York, London, 1963) Ch. 17, p. 793.
25. A. GUINIER, and H. LAMBOT, *Compt. Rend.* 227 (1948) 74.
26. J. W. CAHN, *Acta Met.* 9 (1961) 795.